Citation: Cell Death and Disease (2011) 2, e221; doi:10.1038/cddis.2011.104

www.nature.com/cddis

OGX-427 inhibits tumor progression and enhances gemcitabine chemotherapy in pancreatic cancer

V Baylot[1,2], C Andrieu[1,2], M Katsogiannou[1,2], D Taieb[1,2], S Garcia[1,2], S Giusiano[1,2], J Acunzo[1,2], J Iovanna[1,2], M Gleave[3], C Garrido[4] and P Rocchi*[,1,2]

Despite many advances in oncology, almost all patients with pancreatic cancer (PC) die of the disease. Molecularly targeted agents are offering hope for their potential role in helping translate the improved activity of combination chemotherapy into improved survival. Heat shock protein 27 (Hsp27) is a chaperone implicated in several pathological processes such as cancer. Further, Hsp27 expression becomes highly upregulated in cancer cells after chemotherapy. Recently, a modified antisense oligonucleotide that is complementary to Hsp27 (OGX-427) has been developed, which inhibits Hsp27 expression and enhances drug efficacy in cancer xenograft models. Phase II clinical trials using OGX-427 in different cancers like breast, ovarian, bladder, prostate and lung are in progress in the United States and Canada. In this study, we demonstrate using TMA of 181 patients that Hsp27 expression and phosphorylation levels increase in moderately differentiated tumors to become uniformly highly expressed in metastatic samples. Using MiaPaCa-2 cells grown both *in vitro* and xenografted in mice, we demonstrate that OGX-427 inhibits proliferation, induces apoptosis and also enhances gemcitabine chemosensitivity *via* a mechanism involving the eukaryotic translation initiation factor 4E. Collectively, these findings suggest that the combination of Hsp27 knockdown with OGX-427 and chemotherapeutic agents such as gemcitabine can be a novel strategy to inhibit the progression of pancreas cancer.

Cell Death and Disease (2011) **2,** e221; doi:10.1038/cddis.2011.104; published online 20 October 2011
Subject Category: Cancer

Pancreatic cancer (PC) remains one of the most deadly and chemoresistant cancers. Multiple studies have evaluated various chemotherapeutic agents, but a few have produced significant improvement in survival.[1] Gemcitabine remains the first-line drug for the treatment of advanced PC, either alone or in combination with other chemotherapeutic agents. However, the inherent resistance of PC to currently available chemotherapeutic agents presents a major challenge.[1–3] Identification of robust new molecular target and relevant pathways to restore sensitivity to chemotherapeutic agents is a top priority.[1] Several mechanisms like STAT3, NF-kappaB and others has been reported to induce gemcitabine resistance in preclinical models.[4,5] However, in clinic, only one study reports <2 weeks of survival improvement with a combination of erlotinib and gemcitabine,[6] highlighting the urgent need to find novel agents against relevant molecular targets to make new treatments.

Heat shock protein 27 (Hsp27) seems to have a crucial role in regulating the balance between cell death and survival. Hsp27 is phosphoactivated during cell stress to form oligomers that prevent aggregation and/or regulate activity and degradation of certain client proteins.[7] Hsp27 expression is increased in a variety of malignancies including prostate[8,9] breast,[10] gastric,[11] ovarian,[12] bladder[13] and pancreas cancer.[14] Furthermore, Hsp27 overexpression has been associated with multi-drug resistance in several cancers[15] like prostate,[9] breast[16] and bladder.[17] Recently, Mori-Iwamoto *et al.*[18] demonstrated that Hsp27 is a biomarker of PC cell's resistance to gemcitabine and its downregulation mediated by interferon-gamma helps in cytotoxic effect of gemcitabine.[19]

Antisense oligonucleotides (ASOs) are powerful tools that specifically hybridize with complementary mRNA regions forming RNA/DNA duplexes to inhibit target gene expression in a sequence-specific manner. Several gene-targeting ASOs in combination with other compounds, such as chemotherapeutic agents, have shown synergistic anti-neoplastic effects in several tumor models. Recently, Hsp27 ASO and short interference RNA (siRNA) were reported to potently inhibit Hsp27 expression in human prostate PC-3 cells with increased caspase-3 cleavage, apoptosis and 87% suppression of cell growth.[8,9,20] A second generation ASO-targeting Hsp27 (OGX-427) is currently tested in phase II clinical trials for prostate, bladder, ovarian, breast and lung cancers in the United States and Canada.[21]

In this study, we have been able to associate Hsp27 expression with bad prognosis in PC patients. Further, we

[1]INSERM, U624 'Stress Cellulaire', Parc Scientifique et Technologique de Luminy, Marseille, France; [2]Aix-Marseille Université, Campus de Luminy, Marseille, France; [3]The Prostate Centre, Vancouver General Hospital, Vancouver, British Columbia, Canada and [4]INSERM, U866, Faculty of Medicine, Dijon, France
*Corresponding author: P Rocchi, INSERM, U624 'Stress Cellulaire', Parc Scientifique et Technologique de Luminy, 163 avenue de Luminy, 13289 Marseille, France. Tel: +33 491 828 808; Fax: +33 491 826 083; E-mail: palma.rocchi@inserm.fr
Keywords: Hsp27; oligonucleotide antisense; pancreas cancer xenograft; eIF4E; gemcitabine chemoresistance
Abbreviations: ASO, antisense oligonucleotide; Hsp27, heat shock Protein 27; eIF4E, eukaryotic translation initiation factor 4E; TMA, tissue microarrays; PC, pancreatic cancer; IPMNP, intraductal papillary mucinous neoplasms of the pancreas; EPT, endocrine pancreas; ADK, adenocarcinoma; WD, well-differentiated; MD, moderately-differentiated; UD, undifferentiated; Meta, metastatic; TCL, total cell lysate; IP, immunoprecipitation; IB, immunoblotting
Received 01.6.11; revised 06.9.11; accepted 16.9.11; Edited by P Salomoni

have explored the role of Hsp27 in PC cell survival using MiaPaCa-2 cells grown both *in vitro* and *in vivo*, and identified a function for Hsp27 in promoting cell growth and chemoresistance.

Results

Hsp27 immunostaining increases in undifferentiated and metastatic human PC. To study the role of Hsp27 in PC, we determine its expression level by immunostaining in 181 pancreas cancer specimens spotted on a tissue microarray (TMA). Hsp27 was found mostly in the cytoplasm of epithelial cells of tumor glands (Figure 1a). More specifically, while Hsp27 staining was absent or weak in less aggressive tumors like intraductal papillary mucinous neoplasms of the pancreas (IPMNP) and endocrine pancreas tumors (EPT), it strongly increased with the loss of differentiation in pancreas adenocarcinomas (ADK). Further, pancreatic tumors from metastatic sites exhibited uniform and highly positive Hsp27 staining in all specimens. The mean intensity scored in percentage of numerous and massive positive cells in IPMNP, EPT, well-differentiated (WD) ADK, moderately/undifferentiated (MD/UD) ADK and metastatic (Meta) samples were 42%, 43%, 68%, 71% and 90%, respectively (Figure 1b).

Overexpression of Hsp27 inhibits gemcitabine-induced apoptosis and promotes tumor growth while Hsp27 downregulation has the opposite effects. In order to determine whether Hsp27 overexpression could be part of PC cell's resistance to the first-line chemotherapeutic agent gemcitabine, we established a MiaPaCa-2 cell line stably expressing human Hsp27 cDNA (MiaPaCa-2-Hsp27). We first confirmed, by western blot, elevated Hsp27 protein levels in MiaPaCa-2-Hsp27 as compared with MiaPaCa-2 stably expressing the empty vector (MiaPaCa-2-Mock) (Figure 2a). After 24 h treatment with gemcitabine (see Materials and Methods) cell viability studies showed that MiaPaCa-2-Hsp27 cells were more resistant to gemcitabine-induced apoptosis compared with Mock cells (Figure 2b). Flow cytometry analysis revealed that Hsp27 overexpression increased the resistance to apoptosis induced by gemcitabine while decreasing the percentage of cells in sub G0 phase (Figure 2c). Conversely, OGX-427, an oligonucleotide antisense of second generation specific for Hsp27 that induced a dose-dependent downregulation of Hsp27 (Figures 2d and e), inhibited cell growth (Figure 2f), induced apoptosis (Figure 2g) and sensitized MiaPaCa-2 cells to gemcitabine (Figure 2h).

OGX-427 inhibits proliferation and sensitizes to gemcitabine *via* inhibition of the eukaryotic translational initiation factor 4E (eIF4E). We recently showed in prostate cancer cells that a relevant pathway through which Hsp27 inhibits apoptosis was by its interaction with eIF4E thereby protecting this translational factor from its degradation.[22] We therefore studied here the effect of OGX-427 treatment in eIF4E stability. We found that in OGX-427-treated MiaPaCa-2 cells, there was a decrease of $\sim$70% in eIF4E protein at 70 nM (Figures 3a and b). Consistent with this result, eIF4E content was increased in MiaPaCa-2-Hsp27 compared with MiaPaCa-2-Mock (Figure 3c). Hsp27 regulated eIF4E protein expression, without affecting its mRNA expression (data not shown) but by inducing a decrease of $\sim$30% in the amount of ubiquitinated eIF4E (Figures 3d and e) thereby inhibiting its proteasomal degradation as we already reported. As Hsp27 has been shown to induce resistance to cell death in other cancer cell models by interacting with different cellular partners[8,23] we studied the relevance of eIF4E in Hsp27-induced resistance to gemcitabine in PC cells. We depleted eIF4E by means of a specific siRNA[22] and studied the protective effect of Hsp27. We found that when eIF4E was depleted, Hsp27 was unable to modify the sensitivity of the cells to gemcitabine, suggesting the relevance of Hsp27-eIF4E association (Figure 3f).

Collectively, the results illustrated in Figure 3 and data previously published by us indicates that Hsp27 levels correlate with those of eIF4E.[22] Further, Hsp27 interacts directly with eIF4E inhibiting its ubiquitination and proteasomal degradation.

Hsp27 association with eIF4E involves its C-terminal region and depends on the phosphorylation of the chaperone. In order to analyze Hsp27-eIF4E interaction, we used Hsp27 deletion mutants previously described by Al-Madhoun *et al*.[24] The C-terminal mutant Hsp27 N1 (1-93) lacks part of the α-crystallin domain, believed to mediate oligomerization of Hsp27.[15] The Hsp27 N2 mutant (1–173) lacks the flexible domain (IXI box) at the C-terminal, believed to be involved in the formation of multiple inter-subunit interactions.[25] Finally, the N-terminal mutant, Hsp27 C1 (93–205), lacks the hydrophobic WDPF domain and the major phosphorylation sites necessary for interacting with other proteins and molecular chaperone function[26] (Figure 4a).

Immunoprecipitation of eIF4E followed by immunoblot analysis with anti-histidine antibody was performed on MiaPaCa-2 cells transiently transfected with constructs carrying wild type (WT) and Hsp27 truncated mutant forms (N1, N2 and C1). As shown in Figure 4b, eIF4E was able to interact with WT-Hsp27 and N2, while hardly no or weak interaction was observed with N1 and C1, respectively. Interestingly, only transfection with N2 protected MiaPaCa-2 pancreatic cells to gemcitabine-induced apoptosis (protection similar to that observed with WT-Hsp27). In contrast, transfection with N1 or C1 sensitizes MiaPaCa-2 pancreatic cells to gemcitabine (Figure 4c). These results suggest that cytoprotection induced by Hsp27 in MiaPaCa-2 cells seems to involve eIF4E interaction.

Phosphorylation of the 3 Serine (Ser) residues of Hsp27 (position 15, 78 and 82), has been shown to modulate Hsp27 functions.[7] To analyze the effect of Hsp27 phosphorylation on its association with eIF4E, we used two phospho-mutants (3D and 3A) of Hsp27 (Figure 5a). The 3D have the three Ser residues replaced by aspartates that mimics the constitutively phosphorylated protein. The 3A has the three Ser residues replaced by alanines that mimic the constitutively dephosphorylated protein. We found that the constitutively phosphorylated 3D mutant bound to eIF4E more efficiently than WT, while the non-phosphorylatable 3A mutant was unable to do so (Figure 5b). Thus, Hsp27 phosphorylation considerably increases eIF4E interaction.

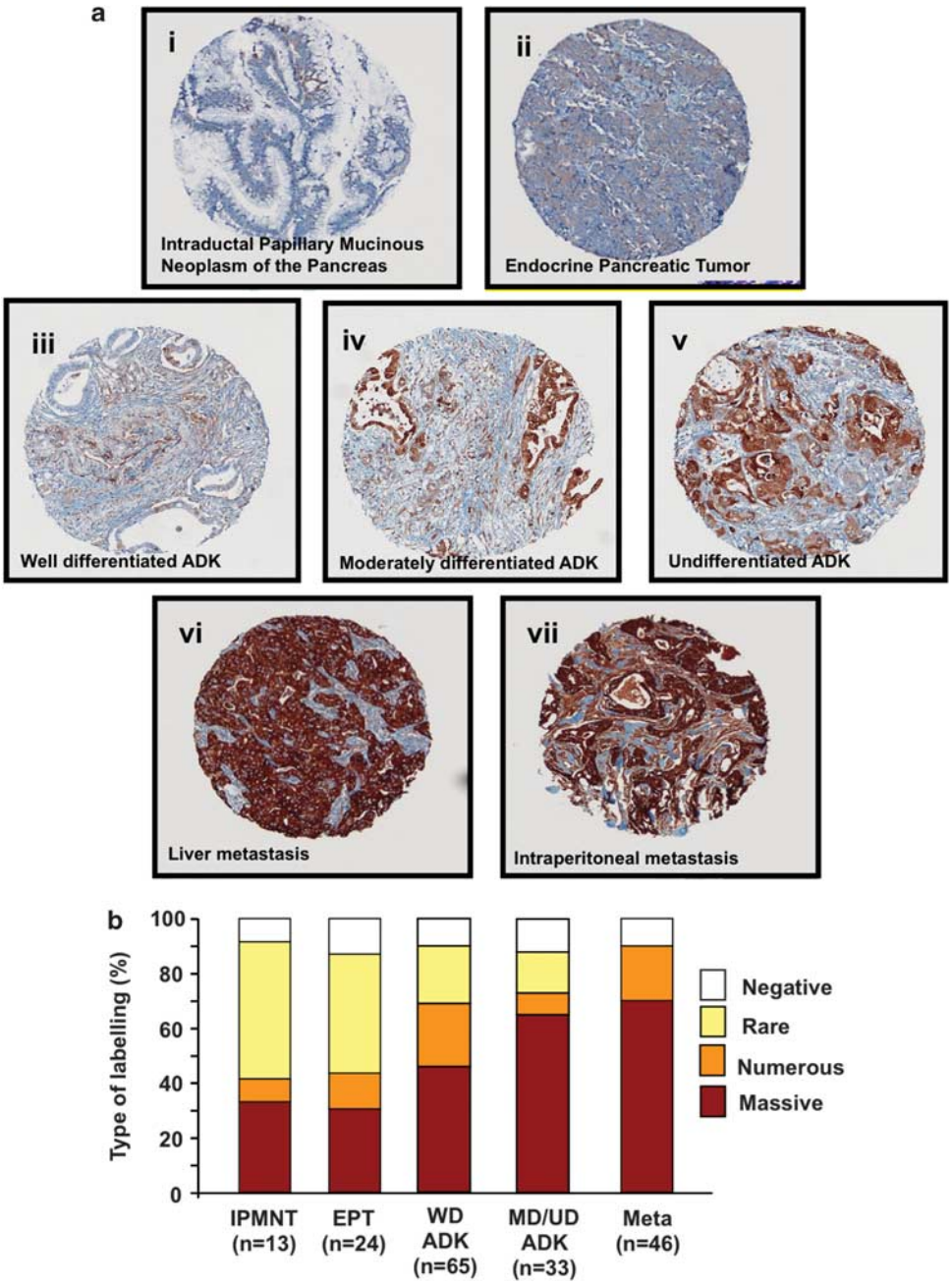

Figure 1 Changes in Hsp27 immunostaining in human pancreas cancer TMA. (**ai** and **aii**) IPMNP and EPT: a few foci of weakly positive cancer cells are visible, but most tumor is not immunoreactive. (**aiii**, **aiv** and **av**) Strong immunoreactivity in WD, MD differentiated and UD ductal adenocarcinoma. (**avi** and **avii**) Sheets of uniformly and intensively reactive tumor cells characteristic of liver and intraperitoneal Meta, respectively. (**b**) Mean Hsp27 staining in human PC TMA. Specimens spotted on the TMA were graded from negative, rare, numerous and massive representing the range of no staining to heavy staining by visual scoring and automated quantitative image analysis by SAMBA 'immune' software. Data from 181 samples were used to calculate average $\pm$S.E. All comparison of stain intensity was made at $\times$200 magnification

Phosphorylated Hsp27: a bad prognosis marker in PC. Previous studies demonstrated that phosphorylation levels of Hsp27 increased in advanced tumors and correlate with treatment resistance.[23,27] Similarly, our results shown above suggest that the phosphorylation of Hsp27 (P-Hsp27) was necessary to confer resistance to gemcitabine. This suggests that P-Hsp27 could be used as bad prognosis factor in PC. To explore this hypothesis, we checked Hsp27 phosphorylation status in human TMA. Figure 6 illustrates that total- and P-Hsp27 are low in WD ductal ADK, strongly increased with the loss of differentiation to become uniformly highly positive in PC from metastatic sites. The increased levels of P-Hsp27 correlated with total-Hsp27 and eIF4E. This result is consistent with recent work published by Taba *et al*.[27] showing that Hsp27 is phosphorylated in gemcitabine-resistant PC. Our results suggest that gemcitabine resistance might involve eIF4E.

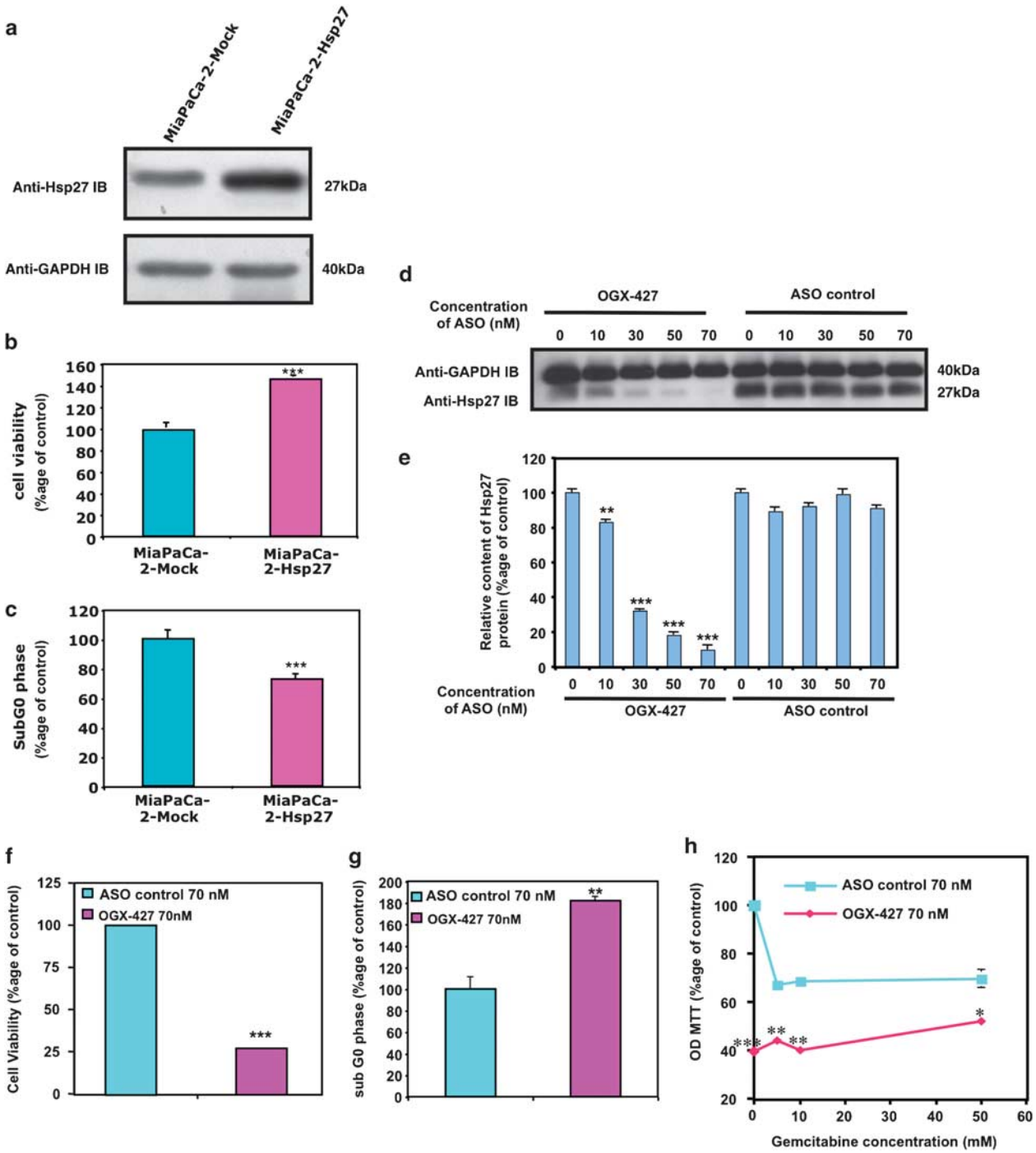

Figure 2 Effect of Hsp27 overexpression and downregulation on chemoresistant MiaPaCa-2 cells survival and apoptosis *in vitro*. (**a**) Western blot analysis of Hsp27 and GAPDH protein levels in MiaPaCa-2 cells stably transfected with empty vector (MiaPaCa-2-Mock) or human Hsp27 (MiaPaCa-2-Hsp27). (**b**) MTT quantification of cell viability of MiaPaCa-2-Hsp27 and -Mock cells and (**c**) apoptosis assay by flow cytometry. The results are expressed in percentage to control (MiaPaCa-2-Mock). (**d**) Western blot analysis of Hsp27 and GAPDH protein levels in MiaPaCa-2 cells transfected with OGX-427 as compared with MiaPaCa-2 ASO control. (**e**) Histograms of average densitometries of Hsp27 protein levels after normalization to GAPDH protein levels by densitometry analysis in MiaPaCa-2 cells after treatment with OGX-427 or ASO control. (**f**) MTT quantification of cell viability of MiaPaCa-2 cells treated with OGX-427 or ASO control. (**g**) Flow cytometry quantification of cell percentage in sub G0 phase of MiaPaCa-2 cells treated with OGX-427 as compared with ASO control. (**h**) MTT quantification of cell viability of MiaPaCa-2 treated with OGX-427 or ASO control combined with different concentrations of gemcitabine. Error bars represent S.E. from three independent experiments. Statistical analysis used *t* test; $^{*}P \leq 0.05$, $^{**}P \leq 0.01$, $^{***}P \leq 0.001$

Anti-cancer effect of OGX-427 *in vivo*. Male nude mice bearing MiaPaCa-2 tumors were randomly selected for treatment with OGX-427 or an ASO control administered alone, or in combination with gemcitabine (see Materials and Methods). Mean tumor volume was similar in all groups before therapy (300–500 mm^3 size). Figures 7a and b show

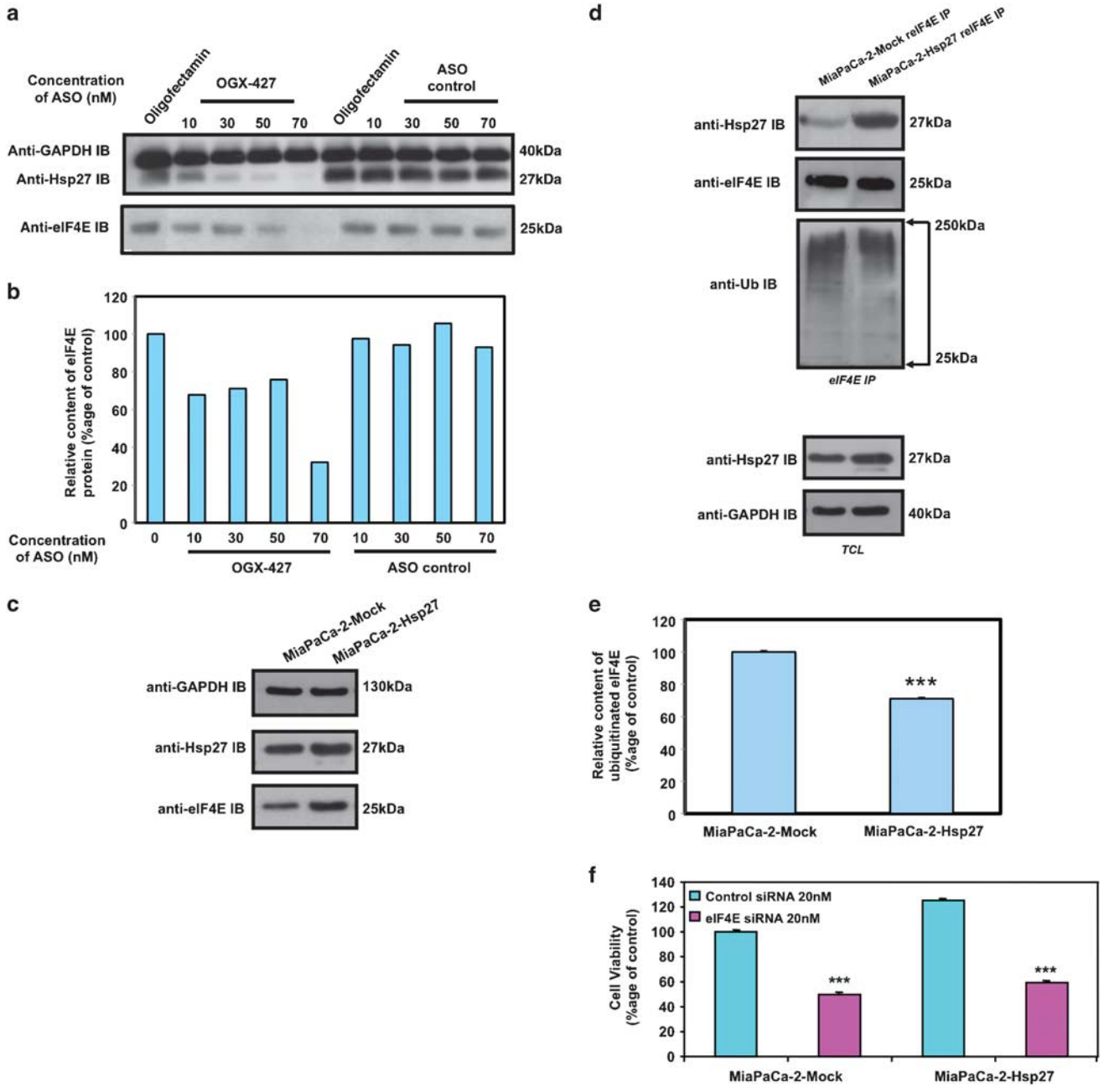

Figure 3 Hsp27 regulates eIF4E and mediates cytoprotection. (**a**) Western blot analysis of Hsp27, eIF4E and GAPDH protein levels in MiaPaCa-2 cells treated with OGX-427 or ASO control. (**b**) Histograms of average densitometries of eIF4E protein level after normalization to GAPDH protein level by densitometry analysis in MiaPaCa-2 cells after treatment with OGX-427 or ASO control. (**c**) Western blot analysis of Hsp27, eIF4E and GAPDH protein levels in MiaPaCa-2 cells stably transfected with empty vector (MiaPaCa-2-Mock) or human Hsp27 (MiaPaCa-2-Hsp27). (**d**) Western blot analysis of Hsp27, ubiquitin and eIF4E protein levels after eIF4E immunoprecipitation (IP) using rabbit anti-eIF4E antibody (reIF4E) in MiaPaCa-2-Mock and MiaPaCa-2-Hsp27 cells. Total cell lysate (TCL) represents proteins from MiaPaCa-2-Mock *vs* MiaPaCa-2-Hsp27 cells, extracted from cultured cells and blotted as control with Hsp27 and GAPDH antibody. (**e**) Histograms of average densitometries of ubiquitine protein levels after normalization to eIF4E protein levels by densitometry analysis in MiaPaCa-2 stably transfected with Hsp27 or Mock control. (**f**) MTT quantification of cell viability of MiaPaCa-2-Mock and MiaPaCa-2-Hsp27 cells treated with 20 nM control- or eIF4E-siRNA and gemcitabine (150 mM). Error bars represent S.E. from three independent experiments. Statistical analysis used *t* test; $^{***}P \leq 0.001$

that OGX-427 monotherapy significantly reduced MiaPaCa-2 tumor volume by up to ~50% from day 14 to 35 ($^{*}P \leq 0.05$; $^{**}P \leq 0.01$). Moreover, treatment with OGX-427, compared with ASO control, significantly enhanced the apoptotic effect of gemcitabine *in vivo*, reducing mean MiaPaCa-2 tumor volume by ~50%, 28 days after initiation of treatment ($^{**}P \leq 0.01$; Figures 7a and b). Under the experimental conditions described above, no adverse effects were observed. Microscopic studies in tumor slides confirmed that the anti-tumor effect of OGX-427 was associated with a

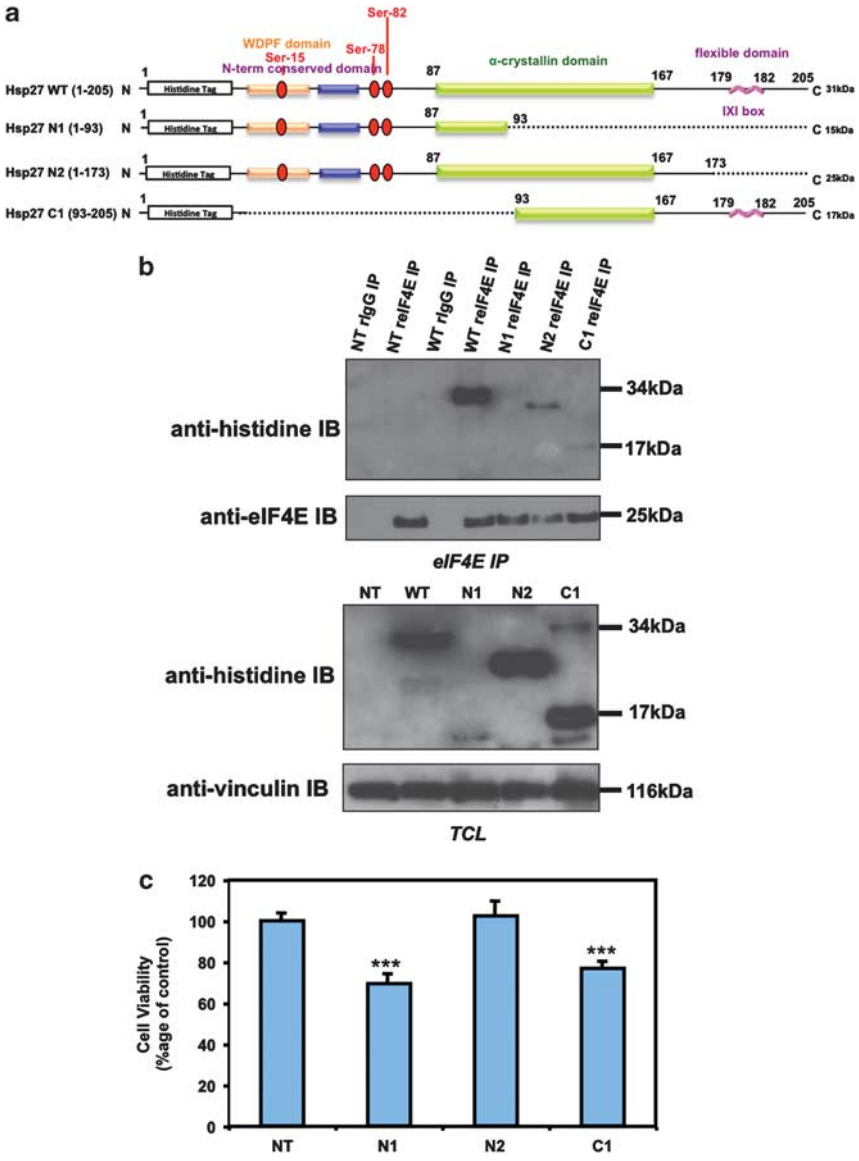

Figure 4 Hsp27 association with eIF4E involves its C-terminal region. (**a**) Schematic representation of Hsp27 structure and deletion mutants used in this study. (**b**) Western blot analysis of histidine and eIF4E protein levels after eIF4E immunoprecipitation (IP) using rabbit anti-eIF4E antibody (reIF4E) or rabbit IgG as control in MiaPaCa-2 cells transiently transfected with WT Hsp27 or truncated mutant forms (N1, N2 and C1) of Hsp27. In the lower panel, western blot analysis of histidine and vinculin levels from total protein extracts (TCL). (**c**) MTT quantification of cell viability of MiaPaCa-2 cells transiently transfected or not with Hsp27 deletion mutants and treated with gemcitabine (150 mM). Error bars, S.E. from three independent experiments. Statistical analysis used *t* test; $^{***}P \leq 0.001$

decrease in Hsp27, eIF4E and ki67 proliferation index and an increase in caspase-3-dependent apoptosis (Figure 7c).

Discussion

Hsp27 expression is induced by various stressors, such as chemotherapy and can act at multiple control points in apoptotic pathways to ensure that stress-induced damage does not inappropriately trigger cell death.[28] Several mechanisms account for the cytoprotective effect of Hsp27, including: (1) chaperone inhibitor of protein misfolding; (2) inhibition of key effectors of the apoptotic machinery at the pre- and post-mitochondrial level[8,20,29] and (3) proteasome-mediated degradation of proteins under stress conditions.[28] Targeting Hsp27 by the second generation ASO, OGX-427, inhibited Hsp27 expression and enhanced drug sensitivity in several xenograft models.[8,9,17] Although mechanisms by which Hsp27 inhibits apoptosis are partially defined, its role in PC growth remains less clear.

In this study, we identified using TMA of 181 specimens that Hsp27 and P-Hsp27 are highly overexpressed in UD PC to become uniformly and highly expressed in metastatic tumors. The highly uniform expression of Hsp27 in metastatic lesions further underscores the association of Hsp27 with the lethal component of the disease. Recently, Mori-Iwamoto *et al.*[18] demonstrated that Hsp27 is a biomarker of resistance of PC cells to gemcitabine and its downregulation mediated by interferon-gamma contributes to gemcitabine cytotoxic

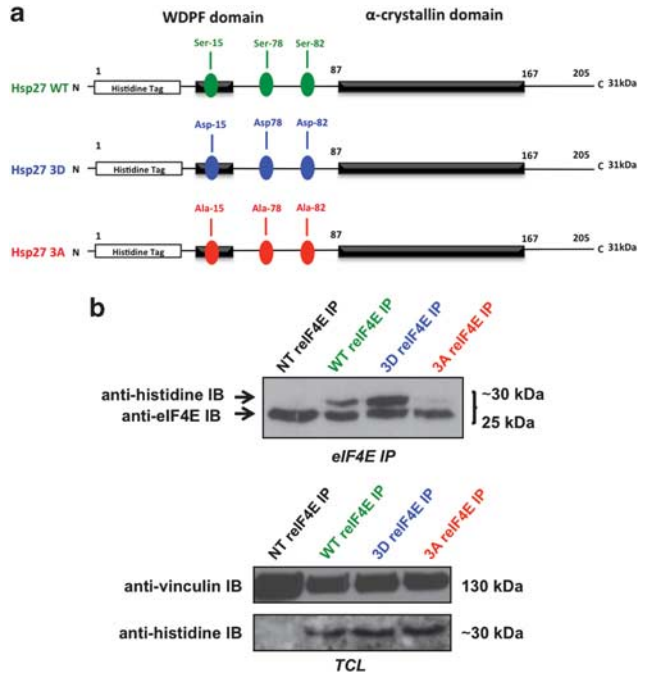

Figure 5 Hsp27-eIF4E interaction depends on Hsp27 phosphorylation. (**a**) Schematic representation of WT and phosphorylation mutants (3D and 3A) of Hsp27 used in this study. (**b**) Western blot analysis of histidine and eIF4E protein levels after eIF4E immunoprecipitation (IP) using rabbit anti-eIF4E antibody (reIF4E) in MiaPaCa-2 cells transiently transfected with Hsp27 WT or 3D (constitutively phosphorylated) and 3A (constitutively dephosphorylated) vectors. In the lower panel, western blot analysis of histidine and vinculin levels from total protein extracts (TCL)

effect.[19] We extend these observations in this work showing that increased Hsp27 levels confer antiapoptotic advantage enhancing gemcitabine apoptosis in chemoresistant MiaPaCa-2 model. Knockdown of Hsp27 in MiaPaCa-2 cells using OGX-427 inhibits proliferation and induces apoptosis *in vitro* and *in vivo*. Furthermore, additive effect was observed when MiaPaCa-2 cells or xenografts were treated with OGX-427 plus gemcitabine.

The mammalian target of rapamycin (mTOR) pathway (eIF4E), has been described to regulate cell survival, and was recently recognized as therapeutic target in several cancers[30] including PC.[31] In most systems, cap-dependent translation depends on eIF4E levels and eIF4E can exert oncogenic effects when overexpressed.[32,33] Previous studies have shown that the mTOR pathway is constitutively active in serum-starved MiaPaCa-2 cells[34] and that eIF4E is upregulated in PC compared with normal cells.[31] Recently, we found that Hsp27 affects eIF4E stability, mediating chemoresistance of advanced prostate cancer.[22] In this report, we demonstrate in MiaPaCa-2 model that changes in Hsp27 expression serve as an upstream regulator of eIF4E. Moreover, we show that Hsp27 and P-Hsp27 levels are directly correlated with eIF4E.

In spite of the importance of eIF4E, little is known about its regulation and role in PC chemoresistance. Transcription of eIF4E gene is induced in response to many stimuli including serum and growth factors.[35] However, mechanisms regulating eIF4E protein expression remain undefined. Othumpangat *et al*.[36] recently reported that eIF4E is ubiquitinated and degraded in a proteasome-dependent manner. Ubiquitin is a low-molecular-weight polypeptide covalently conjugated to lysine residues in target proteins that serve as signal for delivery to and proteolysis by the proteasome.[37] The ubiquitin–proteasome pathway is an important factor controlling the expression and activity of regulatory proteins, such as transcription factors, cell cycle regulators and signal transduction proteins.[38] We recently showed in prostate cancer model that the ubiquitin–proteasome pathway regulates the turnover of eIF4E and cell proliferation. We reported that eIF4E complexes with Hsp27 that induced androgen withdrawal and paclitaxel chemoresistance.[22] Here we demonstrated Hsp27-eIF4E interaction contributes to the overall gemcitabine resistance in MiaPaCa-2 cells and this interaction is favored by phosphorylation of Hsp27.

In summary, the results of this study support the hypothesis that increased Hsp27 in UD and metastatic PC is an adaptive response enhancing cell survival. Hsp27 silencing using OGX-427 alters eIF4E signaling, enhances apoptosis, potentiates gemcitabine activity and offers a new treatment strategy to delay progression of PC. These results provide preclinical proof of principle for the use of OGX-427 as a novel therapeutic strategy in the treatment of PC.

Materials and Methods

Pancreas tissue specimens. Archival resection specimens from 181 patients were studied. Tissue fragments were processed in the Pathology Department, Hôpital Nord (SG). All samples used for TMA construction were fixed in buffered formalin and paraffin embedded. Differentiation and pathological staging were assessed by histological examination according to criteria defined by Kloppel *et al*.[39] Histopathological diagnoses were: IPMNP ($n=13$), EPT ($n=24$), ductal ADK ((WD; $n=65$), (MD; $n=12$) and (UD; $n=21$)) and Meta of pancreatic ductal ADK (peritoneal $n=25$, liver $n=21$).

TMA analysis. TMA were prepared as previously described.[40] For each tumor, two representative tumor areas were delineated by circling within tissue sections appropriate areas with a permanent black pen on hematoxylin- and eosin-stained paraffin sections to guide the punches of cores. Cores were sampled using the ALPHELYS Arraying Device (ALPHELYS, Plaisir, France). Core cylinders of 0.6 mm diameter, punched from the donor block, were then deposited in the recipient paraffin block. TMA sections (4 mm thick) were cut 24 h before immunohistochemical (IHC) processing.

Immunostaining. The IHC procedure was performed with a Ventana Benchmark autostainer (Ventana, Illkirch, France) using the manufacturer procedure and kit as previously reported.[40] Slides were incubated for 32 min at 37°C with specific antibodies from Nova Castra (Newcastle, UK) for total Hsp27, stressgen for the phospho Hsp27 (P-Hsp27) and Cell Signaling technology, Inc. (Danvers, MA, USA) for eIF4E at the concentration of 1/100 in 1% BSA primary antibodies.

Scoring of Hsp27 staining. TMA analysis using the SAMBA 2050 automated device (TRIBVN/SAMBA Technologies, Chatillon, France) was performed according to the protocol previously described.[40] SAMBA 'immuno' software was applied. Several parameters per core were computed: the area of counterstaining, the ratio (as percentage) of the positive area *vs* counterstained areas and a quick score (percentage of positive area mean optical density (OD)). OD was evaluated on a scale of grey levels (arbitrary units) ranging from 0 to 255. The computation of each parameter obtained provided numerical values consisting of continuous variables for statistical tests.

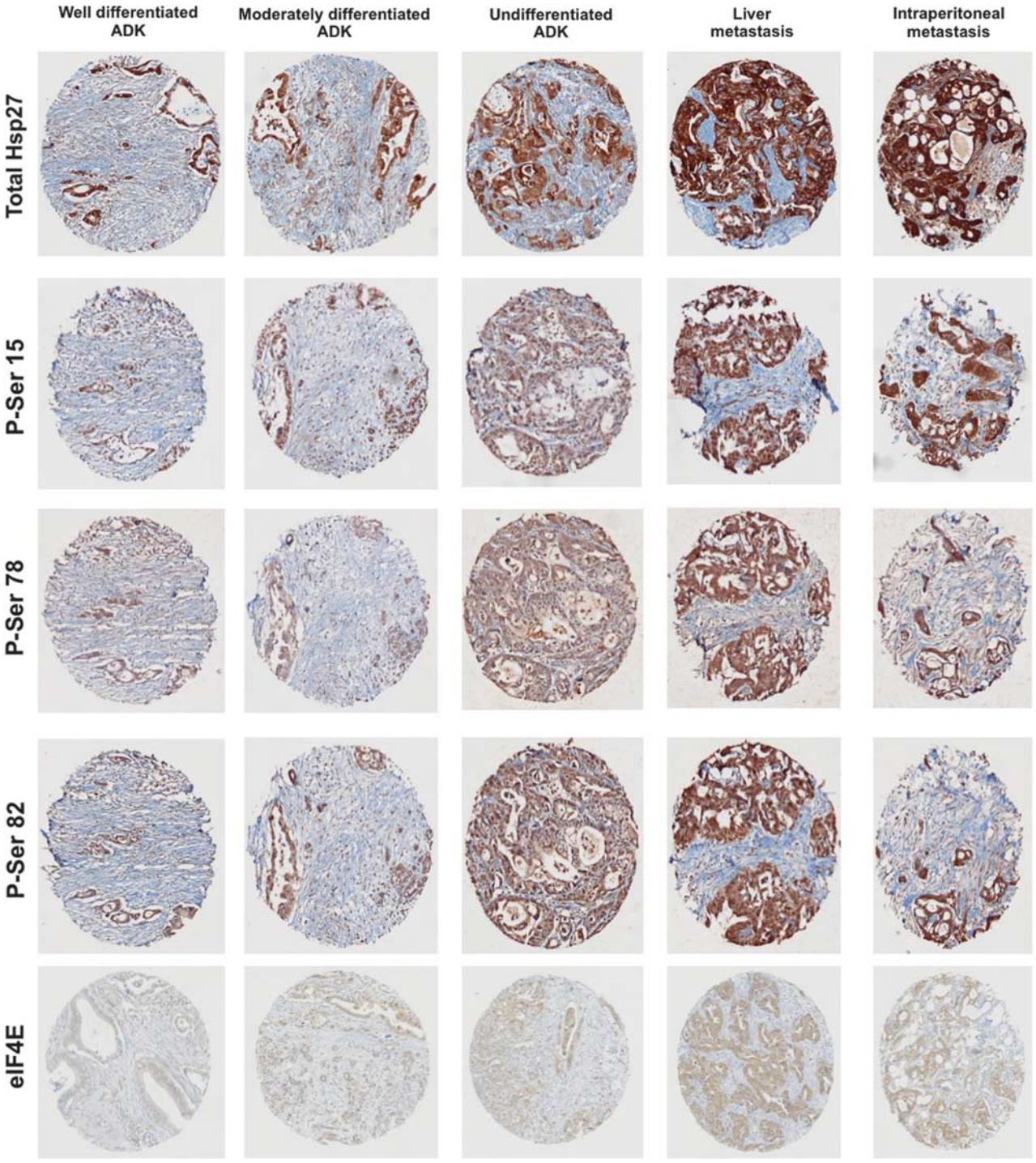

Figure 6 Total Hsp27, phospho-Hsp27 and eIF4E levels in PC tumors. Immunohistochemistry analysis for Hsp27, P-Hsp27 and eIF4E in human pancreas cancer tumors. Specimens from well-differentiated, moderately-differentiated, undifferentiated ADK and metastasis (liver, intraperitoneal) were stained with phospho-serine-15 (P-Ser 15), -78 (P-Ser 78) and -82 (P-Ser 82) Hsp27, total Hsp27 or eIF4E in back to back sections

Tumor cell line. The human chemoresistant PC cell line MiaPaCa-2 obtained from the American Type Culture Collection was maintained in Dulbecco's Modified Eagle Medium (DMEM, Life Technologies, Inc., Gaithersburg, MD, USA) supplemented with 10% fetal calf serum. Cells were routinely grown in 50 ml flasks at 37°C in a humidified 5% CO_2–95% air atmosphere.

Lentiviral Infection of MiaPaCa-2 cells with Hsp27. The full-length cDNA for human Hsp27 was sub cloned into the lentiviral vector pHR'-CMV-EGFP at the *BamH*I and *Xho*I sites. Two vectors were created for this study: pHR'-CMV-Hsp27 (Hsp27) and pHR'-CMV (Mock) as previously described.[8]

Chemotherapeutic agent. Gemcitabine (Gemzar, Lilly Pharmaceutical Company, Suresnes, France) was kindly provided by Dr. Muracciole X (Timone Hospital, Marseilles, France).

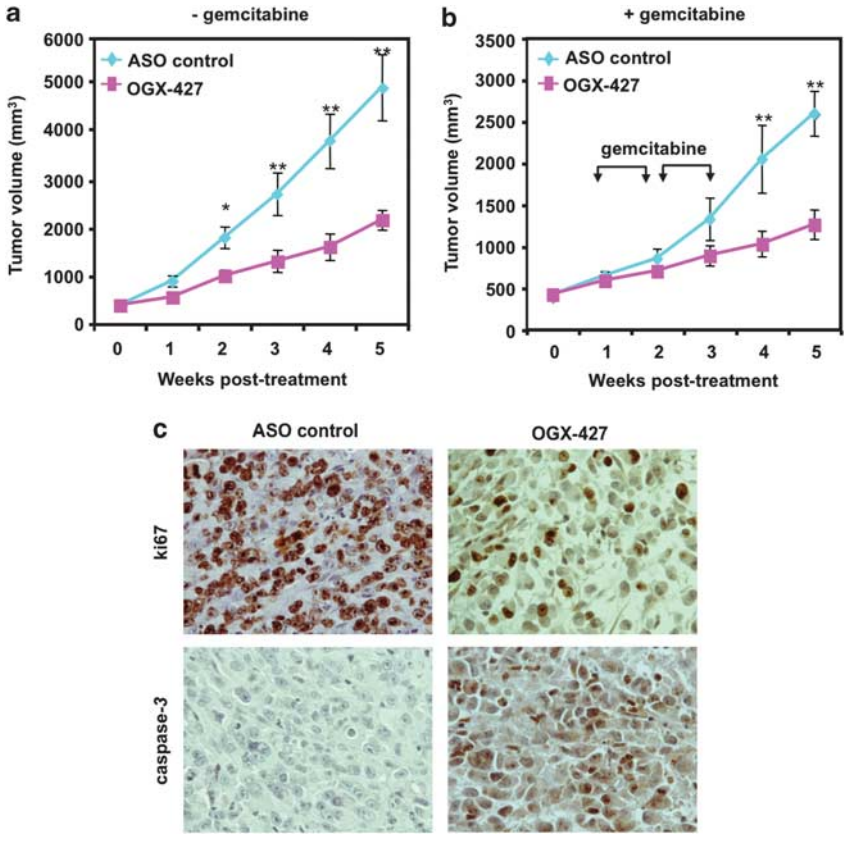

Figure 7 Anti-cancer effect of OGX-427 on MiaPaCa-2 tumor growth and gemcitabine sensitivity *in vivo*. (**a**) and (**b**) MiaPaCa-2 tumor volume measurement (length × width × depth × 0.5236) in 40 nude randomly selected for treatment with OGX-427 or ASO control. When MiaPaCa-2 tumors reached 300–500 mm^3, OGX-427 or ASO control were injected i.p. for 5 weeks for OGX-427 (**a** and **b**) (see Materials and Methods section). Points represent mean tumor volume in each experimental group containing 10 mice; Error bars represent S.E. Statistical analysis used *t* test; $^*P \leq 0.05$, $^{**}P \leq 0.01$. (**c**) IHC staining of MiaPaCa-2 tumor xenografts. Tumors were resected and processed for histological analysis as previously described in Materials and Methods sections. Tissue sections were stained with antibodies to ki67 and cleaved caspase-3

ASO and siRNA sequences and treatment. Hsp27 ASO sequences were manufactured by ISIS Pharmaceuticals (Carlsbad, CA, USA) and supplied by OncoGenex Technologies (Vancouver, British Columbia, Canada) as previously described.[17] The eIF4E siRNA was the Hs_eIF4E_1_HP validated siRNA from Qiagen (Courtaboeuf, France). The control siRNA was from the same source. Plated cells were treated with indicated siRNA or ASO concentrations according to the protocol previously described.[22]

Hsp27 deletion and phosphorylation mutant's transfection. Histidine-tagged (His-tag) Hsp27 WT and three deletion mutants (N1, N2 and C1) in pcDNA4 containing His-tag epitope at N-terminal of the inserted fragment[24] were kindly provided by Pr O'Brien (Ottawa University, Ontario, Canada). The phosphorylation mutants (3D and 3A) in pDEST26 (Invitrogen, Cergy Pontoise, France) containing His-tag at N-terminal of the inserted fragment were obtained after a gateway recombination with the phosphorylation mutants in pENTR kindly provided by Dr. William Gerthoffer (University of South Alabama, USA). MiaPaCa-2 cells were transfected with 10 μg WT, deletion or phosphorylation mutants using Fugene reagent (Roche Diagnostics GmbH, Mannheim, Germany) according to the manufacturer's instructions. Cleared lysates were obtained 48 h post transfection according to our previous experiments.[9]

***In vitro* mitogenic assay.** The *in vitro* growth effects were assessed in 12-well microtiter plates using the 3-(4,5-dimethylthiazol-2-yl)-2,5-diphenyl tetrazolium bromide (MTT) assay as previously described.[9] MiaPaCa-2-Mock and -Hsp27 cells were treated with 150 mM gemcitabine, and MTT assays were performed after 24 h. Wild-type MiaPaCa-2 cells were treated once daily with 70 nM OGX-427 for 2 days and MTT assays were performed 72 h after OGX-427 treatment. MiaPaCa-2 cells, transiently transfected or not with Hsp27 deletion mutants, were treated with gemcitabine during 48 h after transfection and cell viability was assayed 72 h later.

Flow cytometry analysis. Flow cytometry of propidium iodide-stained nuclei was performed as described previously.[9] Briefly, MiaPaCa-2-Mock and -Hsp27 cells were treated with 150 mM gemcitabine. After 24 h, cells were analyzed for relative DNA content on a dual laser flow cytometer (Beckman Coulter Epics Elite, Beckman Inc., Miami, FL, USA). MiaPaCa-2 cells were treated once daily with OGX-427 for 2 days, and flow cytometry assays were performed 24 h after OGX-427 treatment.

Western blot analysis. Western blot analysis was performed as described previously[9] using 1 : 5000 rabbit anti-Hsp27 polyclonal antibody (Assay designs, MI, USA), 1 : 1000 mouse anti-Hsp27 monoclonal antibody (Assay designs), 1 : 1000 rabbit anti-eIF4E polyclonal antibody (Cell Signaling technology, Inc.), 1 : 500 mouse anti-ubiquitin monoclonal antibody (Santa Cruz Biotechnology, Inc., Delaware, CA, USA) and 1 : 3000 mouse monoclonal histidine antibody (Sigma, St. Louis, MO, USA). Loading levels were normalized using 1 : 5000 rabbit anti-GAPDH polyclonal antibody or 1 : 2500 mouse anti-vinculin monoclonal antibody (Sigma).

Immunoprecipitation. Cleared lysates with adjusted protein concentration (Protein assay, BioRad, Marnes-la-Coquette, France) were used for immunoprecipitation with rabbit anti-Hsp27 antibody (Assay designs), rabbit anti-eIF4E antibody (Cell Signaling technology, Inc.), rabbit IgG (rIgG; Millipore, Billerica, MA, USA) at 4°C. Immune complexes were precipitated following 1-h incubation with 30 μl true blot rabbit beads (eBiosciences SAS, Paris, France) at 4°C. Complexes were suspended in protein sample buffer (BioRad) and boiled for 5 min.

Western Blot analysis was performed as previously described[9] with secondary anti-mouse and anti-rabbit true blot HRP-conjugated antibodies (eBiosciences).

Assessment of *in vivo* tumor growth. For *in vivo* study, 10^6 MiaPaCa-2 cells were inoculated s.c. with 0.1 ml of Matrigel (Becton Dickinson Labware, Franklin Lakes, NJ, USA) in the flank region of 4–5 week-old male athymic nude mice (Harlan Sprague Dawley, Inc. Indianapolis, IN) *via* 27-gauge needle. Tumors were measured weekly and their volumes were calculated by the formula length $\times$ width $\times$ depth $\times$ 0.5236. When MiaPaCa-2 tumors reached 300–500 mm^3, mice were randomly selected for treatment with OGX-427 alone, ASO control alone, OGX-427 and ASO control plus gemcitabine. Each experimental group consisted of 10 mice. After randomization, 10 mg/kg OGX-427 or ASO control was injected i.p. three times a week for 5 weeks. A total of 150 mg/kg gemcitabine was administrated i.v. every 3 days from day 7 to 14 and from day 21 to 28. Data points were expressed as average tumor volume levels $\pm$ S.E.

Immunohistochemical determination of Ki67 and caspase-3 for proliferation index and *in situ* apoptosis. The expression of Ki67 and caspase-3 was detected in histological sections of tumor xenografts. Sections were cut from formalin-fixed and paraffin-embedded tissue blocks. The primary rabbit monoclonal anti-ki67 (1/200) and caspase-3 (1/50) antibodies from Epitomic, Inc. (Burlingame, CA, USA) was added. The sections were incubated with diaminobenzidine substrate as chromogen.

Statistical analysis. All the results were expressed as mean $\pm$ S.E. Statistical analysis was performed by one-way ANOVA followed by Fisher's protected least significant difference test (Statview 512, Brain Power Inc., Calabases, CA, USA). $P \leq 0.05$ was considered significant (*); $P \leq 0.01$ (**); $P \leq 0.001$ (***).

Conflict of Interest

The University of British Columbia has submitted patent applications, listing Dr. Gleave and Dr. Rocchi as inventors, on the antisense sequence described in this paper. This patent has been licensed to OncoGenex Technologies, a Vancouver-based biotechnology company that Dr Gleave has founding shares in.

Acknowledgements. We thank Pr Edward O'Brien (Ottawa University, Canada) for providing the Hsp27 pcDNA4/HIS deletion mutant vectors. We thank Dr. William Gerthoffer (South Alabama University, USA) for providing the Hsp27 pENTR phosphorylation mutant vectors. We also thank Virginia Yago (Prostate Centre, Canada) for her excellent technical assistance in animal and laboratory experimentation. We thank Marie-Noëlle Lavaut for her excellent technical help for the immunohistochemistry. This work was supported from grants by l'Institut National de la Santé et de la Recherche Médicale (INSERM), l'Association pour la Recherche sur le Cancer (ARC), l'Association pour la Recherche sur les Tumeurs de la Prostate (ARTP), l'institut national du cancer (InCa), la ligue contre le cancer, l'agence nationale de la recherche (ANR) and le ministère de la recherche et de l'enseignement supérieur.

1. Van Laethem JL, Verslype C, Iovanna JL, Michl P, Conroy T, Louvet C *et al.* New strategies and designs in pancreatic cancer research: consensus guidelines report from a European expert panel. *Ann Oncol* 2011; e-pub ahead of print 1 August 2011.
2. Conroy T, Desseigne F, Ychou M, Bouche O, Guimbaud R, Becouarn Y *et al.* FOLFIRINOX versus gemcitabine for metastatic pancreatic cancer. *N Engl J Med* 2011; **364**: 1817–1825.
3. Cunningham D, Chau I, Stocken DD, Valle JW, Smith D, Steward W *et al.* Phase III randomized comparison of gemcitabine versus gemcitabine plus capecitabine in patients with advanced pancreatic cancer. *J Clin Oncol* 2009; **27**: 5513–5518.
4. Egloff AM, Grandis JR. Response to combined molecular targeting: defining the role of P-STAT3. *Clin Cancer Res* 2011; **17**: 393–395.
5. Wang SJ, Gao Y, Chen H, Kong R, Jiang HC, Pan SH *et al.* Dihydroartemisinin inactivates NF-kappaB and potentiates the anti-tumor effect of gemcitabine on pancreatic cancer both *in vitro* and *in vivo*. *Cancer Lett* 2010; **293**: 99–108.
6. Moore MJ, Goldstein D, Hamm J, Figer A, Hecht JR, Gallinger S *et al.* Erlotinib plus gemcitabine compared with gemcitabine alone in patients with advanced pancreatic cancer: a phase III trial of the National Cancer Institute of Canada Clinical Trials Group. *J Clin Oncol* 2007; **25**: 1960–1966.
7. Garrido C. Size matters: of the small HSP27 and its large oligomers. *Cell Death Differ* 2002; **9**: 483–485.
8. Rocchi P, Beraldi E, Ettinger S, Fazli L, Vessella RL, Nelson C *et al.* Increased Hsp27 after androgen ablation facilitates androgen-independent progression in prostate cancer via signal transducers and activators of transcription 3-mediated suppression of apoptosis. *Cancer Res* 2005; **65**: 11083–11093.
9. Rocchi P, So A, Kojima S, Signaevsky M, Beraldi E, Fazli L *et al.* Heat shock protein 27 increases after androgen ablation and plays a cytoprotective role in hormone-refractory prostate cancer. *Cancer Res* 2004; **64**: 6595–6602.
10. Love S, King RJ. A 27 kDa heat shock protein that has anomalous prognostic powers in early and advanced breast cancer. *Br J Cancer* 1994; **69**: 743–748.
11. Huang Q, Ye J, Chen W, Wang L, Lin W, Lin J *et al.* Heat shock protein 27 is over-expressed in tumor tissues and increased in sera of patients with gastric adenocarcinoma. *Clin Chem Lab Med* 2010; **48**: 263–269.
12. Langdon SP, Rabiasz GJ, Hirst GL, King RJ, Hawkins RA, Smyth JF *et al.* Expression of the heat shock protein HSP27 in human ovarian cancer. *Clin Cancer Res* 1995; **1**: 1603–1609.
13. Lebret T, Watson RW, Molinie V, O'Neill A, Gabriel C, Fitzpatrick JM *et al.* Heat shock proteins HSP27, HSP60, HSP70, and HSP90: expression in bladder carcinoma. *Cancer* 2003; **98**: 970–977.
14. Melle C, Ernst G, Escher N, Hartmann D, Schimmel B, Bleul A *et al.* Protein profiling of microdissected pancreas carcinoma and identification of HSP27 as a potential serum marker. *Clin Chem* 2007; **53**: 629–635.
15. Ciocca DR, Oesterreich S, Chamness GC, McGuire WL, Fuqua SA. Biological and clinical implications of heat shock protein 27,000 (Hsp27): a review. *J Natl Cancer Inst* 1993; **85**: 1558–1570.
16. Fujita R, Ounzain S, Wang AC, Heads RJ, Budhram-Mahadeo VS. Hsp-27 induction requires POU4F2/Brn-3b TF in doxorubicin-treated breast cancer cells, whereas phosphorylation alters its cellular localisation following drug treatment. *Cell Stress Chaperones* 2011; **16**: 427–439.
17. Kamada M, So A, Muramaki M, Rocchi P, Beraldi E, Gleave M. Hsp27 knockdown using nucleotide-based therapies inhibit tumor growth and enhance chemotherapy in human bladder cancer cells. *Mol Cancer Ther* 2007; **6**: 299–308.
18. Mori-Iwamoto S, Kuramitsu Y, Ryozawa S, Mikuria K, Fujimoto M, Maehara S *et al.* Proteomics finding heat shock protein 27 as a biomarker for resistance of pancreatic cancer cells to gemcitabine. *Int J Oncol* 2007; **31**: 1345–1350.
19. Mori-Iwamoto S, Taba K, Kuramitsu Y, Ryozawa S, Tanaka T, Maehara S *et al.* Interferon-gamma down-regulates heat shock protein 27 of pancreatic cancer cells and helps in the cytotoxic effect of gemcitabine. *Pancreas* 2009; **38**: 224–226.
20. Rocchi P, Jugpal P, So A, Sinneman S, Ettinger S, Fazli L *et al.* Small interference RNA targeting heat-shock protein 27 inhibits the growth of prostatic cell lines and induces apoptosis via caspase-3 activation *in vitro*. *BJU Int* 2006; **98**: 1082–1089.
21. Hirte HW Higano CS, Gleave ME, Chi KN. Phase I trial of OGX-427, a 2′methoxyethyl antisense oligonucleotide (ASO), against Hsp27: final results. *J Clin Oncol* 2010; **28** (15S) (suppl; abstr 3077).
22. Andrieu C, Taieb D, Baylot V, Ettinger S, Soubeyran P, De-Thonel A *et al.* Heat shock protein 27 confers resistance to androgen ablation and chemotherapy in prostate cancer cells through eIF4E. *Oncogene* 2010; **29**: 1883–1896.
23. Zoubeidi A, Zardan A, Wiedmann RM, Locke J, Beraldi E, Fazli L *et al.* Hsp27 promotes insulin-like growth factor-I survival signaling in prostate cancer via p90Rsk-dependent phosphorylation and inactivation of BAD. *Cancer Res* 2010; **70**: 2307–2317.
24. Al-Madhoun AS, Chen YX, Haidari L, Rayner K, Gerthoffer W, McBride H *et al.* The interaction and cellular localization of HSP27 and ERbeta are modulated by 17beta-estradiol and HSP27 phosphorylation. *Mol Cell Endocrinol* 2007; **270**: 33–42.
25. Lelj-Garolla B, Mauk AG. Self-association of a small heat shock protein. *J Mol Biol* 2005; **345**: 631–642.
26. Lindquist S, Craig EA. The heat-shock proteins. *Annu Rev Genet* 1988; **22**: 631–677.
27. Taba K, Kuramitsu Y, Ryozawa S, Yoshida K, Tanaka T, Maehara S *et al.* Heat-shock protein 27 is phosphorylated in gemcitabine-resistant pancreatic cancer cells. *Anticancer Res* 2010; **30**: 2539–2543.
28. Garrido C, Brunet M, Didelot C, Zermati Y, Schmitt E, Kroemer G. Heat shock proteins 27 and 70: anti-apoptotic proteins with tumorigenic properties. *Cell Cycle* 2006; **5**: 2592–2601.
29. Garrido C, Schmitt E, Cande C, Vahsen N, Parcellier A, Kroemer G. HSP27 and HSP70: potentially oncogenic apoptosis inhibitors. *Cell Cycle* 2003; **2**: 579–584.
30. Graff JR, Konicek BW, Carter JH, Marcusson EG. Targeting the eukaryotic translation initiation factor 4E for cancer therapy. *Cancer Res* 2008; **68**: 631–634.
31. Mishra R, Miyamoto M, Yoshioka T, Ishikawa K, Matsumura Y, Shoji Y *et al.* Adenovirus-mediated eukaryotic initiation factor 4E binding protein-1 in combination with rapamycin inhibits tumor growth of pancreatic ductal adenocarcinoma *in vivo*. *Int J Oncol* 2009; **34**: 1231–1240.
32. Mamane Y, Petroulakis E, Rong L, Yoshida K, Ler LW, Sonenberg N. eIF4E–from translation to transformation. *Oncogene* 2004; **23**: 3172–3179.
33. Richter JD, Sonenberg N. Regulation of cap-dependent translation by eIF4E inhibitory proteins. *Nature* 2005; **433**: 477–480.
34. Grewe M, Gansauge F, Schmid RM, Adler G, Seufferlein T. Regulation of cell growth and cyclin D1 expression by the constitutively active FRAP-p70s6K pathway in human pancreatic cancer cells. *Cancer Res* 1999; **59**: 3581–3587.

35. Rosenwald IB, Rhoads DB, Callanan LD, Isselbacher KJ, Schmidt EV. Increased expression of eukaryotic translation initiation factors eIF-4E and eIF-2 alpha in response to growth induction by c-myc. *Proc Natl Acad Sci USA* 1993; **90**: 6175–6178.
36. Othumpangat S, Kashon M, Joseph P. Eukaryotic translation initiation factor 4E is a cellular target for toxicity and death due to exposure to cadmium chloride. *J Biol Chem* 2005; **280**: 25162–25169.
37. Pickart CM. Ubiquitin enters the new millennium. *Mol Cell* 2001; **8**: 499–504.
38. Mitchell BS. The proteasome—an emerging therapeutic target in cancer. *N Engl J Med* 2003; **348**: 2597–2598.
39. Kloppel G. Staging of pancreatic carcinoma. *Int J Pancreatol* 1991; **8**: 203–204.
40. Garcia S, Dales JP, Jacquemier J, Charafe-Jauffret E, Birnbaum D, Andrac-Meyer L *et al.* c-Met overexpression in inflammatory breast carcinomas: automated quantification on tissue microarrays. *Br J Cancer* 2007; **96**: 329–335.